NUMERICAL SIMULATION OF TRACER DISPLACEMENT IN OIL RESERVOIRS

Francisco D. Rocamora Jr.
Instituo de Estudos Avançados - IEAv/CTA
Rod. dos Tamoios, Km 5,5, 12231-970 - São José dos Campos - SP, Brazil
E-mail: rocamora@mec.ita.br

Marcos Heinzelmann Junqueira Pedras
Instituto de Pesquisa e Desenvolvimento IP&D, UNIVAP
Av. Shishima Hifumi, 2911-São José dos Campos-SP, Brazil
E-mail: pedras@univap.br

Marcelo J.S. De-Lemos*
Departamento de Energia – IEME, Instituto Tecnológico de Aeronáutica – ITA, 12228-900 - São José dos Campos - SP, Brazil
Tel: +55-12 3947.5860, Fax: +55-12-3947.5842
* Corresponding author. E-mail: delemos@mec.ita.br

Abstract. *In this article, a two-dimensional time-dependent study of the concentration of a tracer injected in a hybrid medium, i.e., a medium composed of several different porous media, as well as clear (unobstructed) regions, is performed using the Finite Volume method and a single computational domain. The mathematical model here employed is based on the 'double-decomposition theory' developed for the treatment of turbulent flow in a rigid, homogeneous and saturated porous medium. The numerical methodology is based on the SIMPLE method of Patankar (1980). Appropriate boundary and interface conditions, similar to the ones proposed by Ochoa-Tapia and Whitaker (1997) and Quintard et al. (1997), are used in order to simulate the tracer behavior in an oil reservoir. A totally implicit scheme is used for the time-dependent problem, which seems to be adequate in view of the velocity range involved. An assessment to the numerical diffusion introduced by the interpolation scheme as well as by the grid refinement is also presented based on a simple geometry.*

Keywords. *Porous Medium, Turbulent heat transfer, Numerical methods*

1. Introduction

In petroleum reservoir engineering tracers have long been used in order to obtain qualitative information of the underground porous medium such as flow barriers, preferential flow direction, linking paths between reservoirs, etc (see, *e.g.*, Almeida and Cotta (1995), Oldenburg and Pruess (2000), and others). As the information supplied by the tracers is fed back into the model, it becomes more and more accurate. In order to be able to correctly interpret this information, it is necessary that the modeler have access to trustable reservoir simulators, knowing beforehand its limitations and weaknesses. This work aims at presenting a macroscopic model, based on the 'double decomposition concept', for turbulent flows in porous media proposed by Pedras and de Lemos (2000)and Pedras and de Lemos (2002), for the transport of a tracer in a petroleum reservoir, which is assumed to be composed of two regions with different permeabilities and one injection and one production wells. Although the turbulence model is not used in the present work due to the geometry considered, it could become necessary if one would like to detail the regions close to the injection or production wells, where the flow suffers significant acceleration. Also, an analysis of the influence of some parameters as, *e.g.*, grid refinement and numerical schemes, on the tracer concentration front is made in order to establish the simulator limitations.

2. Flow geometry

The geometry considered in this work is based on the one presented by Wendland *et al*. (2001) and is shown in Figure 1. According to the figure, the tracer is injected at the lower left corner and the fluid is extracted from the upper right corner, configuring a *five-spot* pattern. At the center of the flow field there is a region with a different permeability. Also, the dimensions of the flow field are shown in the figure, including the inlet and outlet regions.

3. Mathematical model

For an incompressible flow through a rigid, homogeneous and saturated porous medium, Pedras and de Lemos (2002), using the 'double decomposition concept', have derived the following macroscopic turbulence flow equations:

Continuity equation -

$$\nabla \cdot \overline{\mathbf{u}}_D = 0 \tag{1}$$
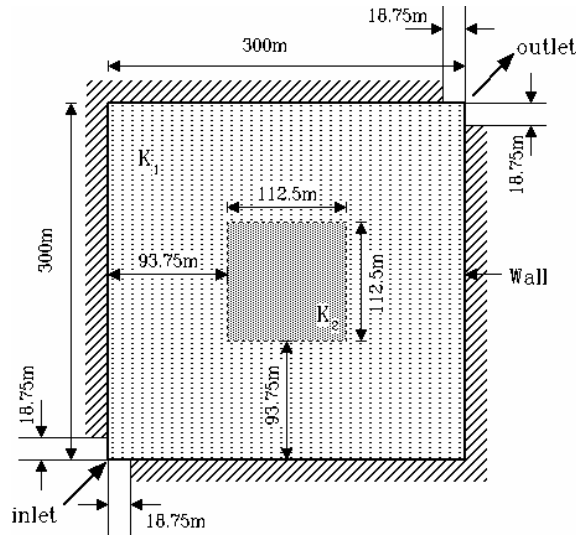
Figure 1 - Flow geometry.

Momentum equation -

$$\rho\left[\frac{\partial \overline{\mathbf{u}}_D}{\partial t}+\nabla\cdot\left(\frac{\overline{\mathbf{u}}_D\,\overline{\mathbf{u}}_D}{\phi}\right)\right]=-\nabla\left(\phi\langle\overline{p}\rangle^i\right)+\mu\nabla^2\overline{\mathbf{u}}_D+\nabla\cdot\left(-\rho\phi\langle\overline{\mathbf{u'u'}}\rangle^i\right)+\phi\rho\mathbf{g}-\left[\frac{\mu\phi}{K}\overline{\mathbf{u}}_D+\frac{c_F\phi\rho|\overline{\mathbf{u}}_D|\,\overline{\mathbf{u}}_D}{\sqrt{K}}\right] \tag{2}$$

where the macroscopic Reynolds' stress tensor is given by:

$$-\rho\phi\langle\overline{\mathbf{u'u'}}\rangle^i=\mu_{t_\phi}2\langle\overline{\mathbf{D}}\rangle^v-\frac{2}{3}\phi\rho\langle k\rangle^i\mathbf{I} \tag{3}$$

and the deformation tensor is given by:

$$\langle\overline{\mathbf{D}}\rangle^v=\frac{1}{2}\left[\nabla\left(\phi\langle\overline{\mathbf{u}}\rangle^i\right)+\left[\nabla\left(\phi\langle\overline{\mathbf{u}}\rangle^i\right)\right]^T\right] \tag{4}$$

Here, μ_{t_ϕ} express the macroscopic Eddy viscosity given as:

$$\mu_{t_\phi}=\rho C_\mu f_\mu\frac{\langle k\rangle^{i\,2}}{\langle\varepsilon\rangle^i} \tag{5}$$

Turbulent kinetic energy equation -

$$\rho\left[\frac{\partial}{\partial t}\left(\phi\langle k\rangle^i\right)+\nabla\cdot\left(\overline{\mathbf{u}}_D\langle k\rangle^i\right)\right]=\nabla\cdot\left[\left(\mu+\frac{\mu_{t_\phi}}{\sigma_k}\right)\nabla\left(\phi\langle k\rangle^i\right)\right]-\rho\langle\overline{\mathbf{u'u'}}\rangle^i:\nabla\overline{\mathbf{u}}_D+C_k\rho\frac{\phi\,k_\phi|\overline{\mathbf{u}}_D|}{\sqrt{K}}-\rho\phi\langle\varepsilon\rangle^i \tag{6}$$

Turbulent kinetic energy dissipation rate -

$$\rho\left[\frac{\partial}{\partial t}\left(\phi\langle\varepsilon\rangle^i\right)+\nabla\cdot\left(\overline{\mathbf{u}}_D\langle\varepsilon\rangle^i\right)\right]=\nabla\cdot\left[\left(\mu+\frac{\mu_{t_\phi}}{\sigma_\varepsilon}\right)\nabla\left(\phi\langle\varepsilon\rangle^i\right)\right]+C_1\left(-\rho\langle\overline{\mathbf{u'u'}}\rangle^i:\nabla\overline{\mathbf{u}}_D\right)\frac{\langle\varepsilon\rangle^i}{\langle k\rangle^i}$$
$$+C_2 f_2 C_k\rho\frac{\phi\,\varepsilon_\phi|\overline{\mathbf{u}}_D|}{\sqrt{K}}-C_2 f_2\rho\phi\frac{\langle\varepsilon\rangle^{i\,2}}{\langle k\rangle^i} \tag{7}$$

Concentration equation -

$$\frac{\partial}{\partial t}\left(\phi\langle C\rangle^i\right)+\nabla\cdot\left(\overline{\mathbf{u}}_D\langle C\rangle^i\right)=\nabla\cdot\left[\underline{\underline{\mathbf{D}}}_{eff}\,\nabla\left(\phi\langle C\rangle^i\right)\right] \tag{8}$$

where the effective diffusion-dispersion tensor, $\underline{\underline{\mathbf{D}}}_{eff}$, was proposed by de Lemos and Mesquita (2003) following similar ideas for the thermal dispersion tensor obtained in Rocamora and de Lemos (2000). A model for it is given by:

$$\underline{\underline{\mathbf{D}}}_{eff}=D_{dif}\,\underline{\underline{\mathbf{I}}}+\underline{\underline{\mathbf{D}}}_t+\underline{\underline{\mathbf{D}}}_{disp}+\underline{\underline{\mathbf{D}}}_{disp,t} \tag{9}$$

In Eq. (9) the tensors $\underline{\underline{D}}_t$, $\underline{\underline{D}}_{disp}$ and $\underline{\underline{D}}_{disp,t}$ are due to turbulence, dispersion and turbulent dispersion, respectively, and will not be taken in to account in the present work. Only the diffusion coefficient for the tracer, D_{dif}, will be considered.

In the equations above the surface volume average quantities are related to the intrinsic average quantities through the porosity ϕ as:

$$\langle \varphi \rangle^v = \phi \langle \varphi \rangle^i \qquad (10)$$

Thus, $\overline{\mathbf{u}}_D = \phi \langle \overline{\mathbf{u}} \rangle^i$ is the surface average fluid velocity or *Darcy*'s velocity. Also, the parameters c_μ, σ_k, σ_ε, $c_{1\varepsilon}$, $c_{2\varepsilon}$ and c_k are model constants whose values are given in Table 1 bellow:

Table 1 - High Reynolds k-ε model constants.

σ_k	σ_ε	c_μ	$c_{1\varepsilon}$	$c_{2\varepsilon}$	c_k
1.0	1.33	0.09	1.44	1.92	0.285

It should be mentioned that the equations presented previously also hold for a clean-medium making $\phi = 1$ and $K \to \infty$.

4. Numerical method

The discretization of the equations is accomplished using the finite volume method in a 2D geometry. The SIMPLE algorithm of Patankar (1980) is used to solve the flow equations. The computational domain is divided in (64x64) cells for the reservoir problem. A totally implicit scheme is used for the time dependent problem with a time step of 1 (one) day. The results are considered converged when the residues are $\leq 10^{-5}$. To assess the numerical diffusion, four grids and three numerical schemes are considered. The grids are (32x5), (64x5), (128x5) and (256x5) for a (300x1) meters channel with symmetry boundary conditions on both sides. The numerical schemes considered are the Up-Wind Scheme (UPS), Central Difference Scheme (CDS), and a Blending Scheme (UPS+CDS).

5. Results and discussion

A summary of the cases analyzed is presented in Table (2). For the whole flow field the porosity is assumed to be uniform, $\phi = 0.2$. The outer region permeability is $K_1 = 10^{-7} \text{m}^2$ and for the central region three values for the permeability K_2 are considered, $K_1/K_2 = 2$, $K_1/K_2 = 10$ and $K_1/K_2 = 10^3$.

Table 2 - Summary of the cases analyzed.

Case #	ϕ	K_1 (m²)	K_1/K_2	D_{dif} (m²/s)
1	0.2	10^{-7}	2	10^{-4}
2	0.2	10^{-7}	10	10^{-4}
3	0.2	10^{-7}	1000	10^{-4}

The fluid properties are given in Table 3.

Table 3 Fluid properties.

ρ (Kg/m³)	1000.0
μ (N s/m²)	10^{-3}

The initial and boundary conditions for the problem are given as follows:
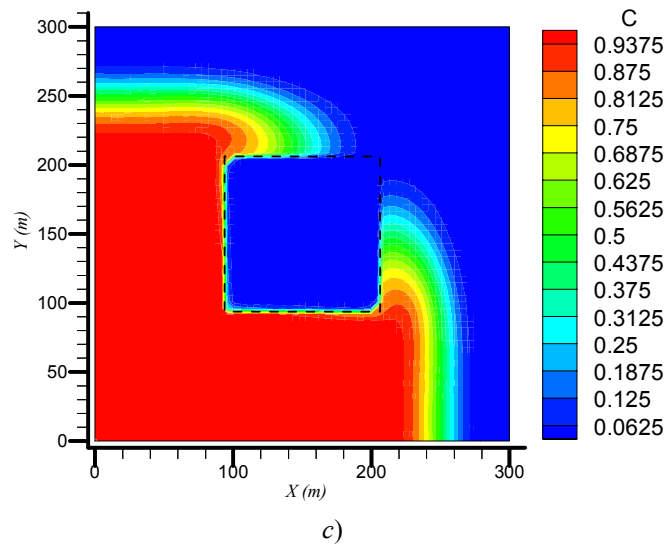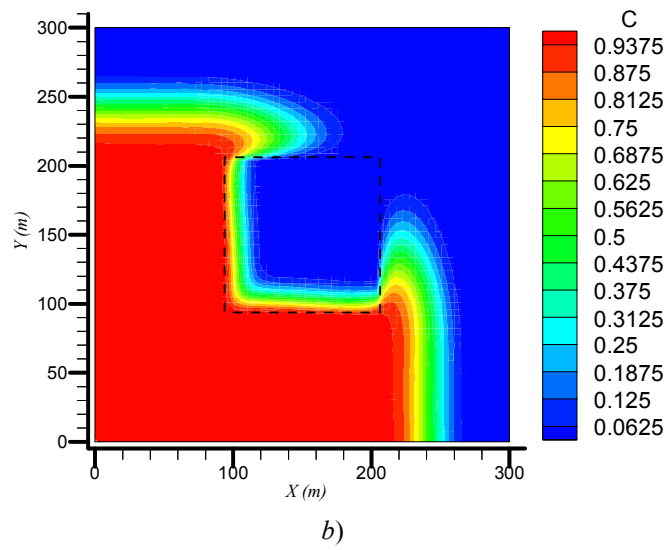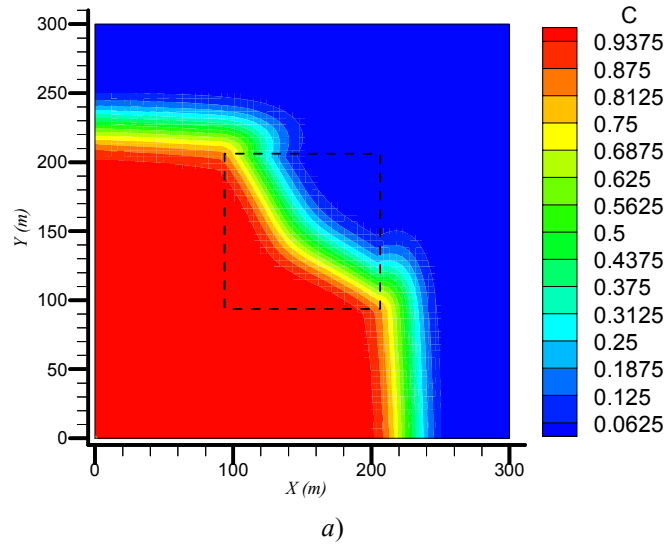
Figure 2 - Concentrations after 800 days continuous injection of tracer. *a*) $K_1/K_2 = 2$; *b*) $K_1/K_2 = 10$; *c*) $K_1/K_2 = 10^3$.

- For the momentum equation:

$\mathbf{n} \cdot \overline{\mathbf{u}}_D = 0$ at the wall, $t \geq 0$

$\mathbf{n} \cdot \overline{\mathbf{u}}_D = -3.2 \times 10^{-6}$ m/s   at the inlet, $t \geq 0$

$\overline{\mathbf{u}}_D = 0$ for the whole domain at $t = 0$

- For the concentration equation:

$$\langle C \rangle^i = 0 \qquad \text{for the whole domain at } t = 0$$

$$\langle C \rangle^i = 1 \qquad \text{at the inlet, } t \geq 0$$

$$\mathbf{n} \cdot \nabla \langle C \rangle^i = 0 \qquad \text{at the wall, } t \geq 0$$

Figure 2 shows the results for the tracer concentration fields for the three cases considered after 800 days continuous tracer injection. Figure 2 *a* shows a high penetration of the tracer into the central region (lower permeability region). This is expected because the permeability ratio for this case, $K_1/K_2 = 2$, is not so high, approaching the homogeneous situation ($K_1/K_2 = 1$).

For the cases 2 and 3, Figures 2 *b* and *c* show a quite different behavior. For case 3, for instance, where the permeability ratio, $K_1/K_2 = 10^3$, represents an extreme heterogeneity, there is almost no penetration of the tracer in the central region.

Figure 3 shows the evolution of the tracer concentration front for several time intervals after the beginning of tracer injection.
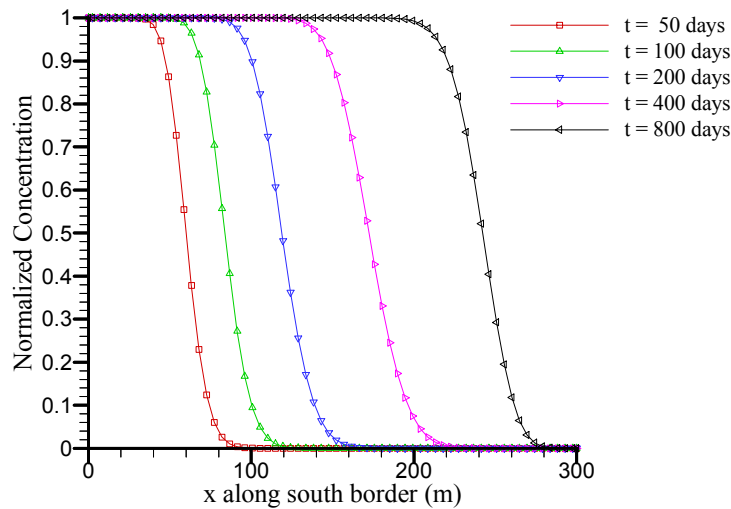
Figure 3 - Normalized Tracer Concentration along the south border (y=2.34m). $K_1/K_2 = 10$.

The results shown in Figure 3 may present some degree of numerical dispersion for the tracer concentration front. As is well known, numerical dispersion may lead to wrong predictions for the tracer breakthrough time and will be addressed next. In order to assess the influence of the grid refinement and the numerical scheme on the concentration front shape, a simple geometry consisting of a channel 300m long and 1m wide was used. At the channel inlet a uniform concentration distribution was assumed and on both sides of the channel symmetry boundary conditions were used. The channel was filled with a porous medium with $\phi = 0.2$ and $K = 10^{-7}\text{m}^2$.

Figure 4 shows the influence of the grid refinement on concentration front shape for a time $t=125$ days after the beginning of injection at $x=0$m. As expected, the more refined the grid the sharper the concentration front is. Unfortunately, this is done at the expense of computing time. A comparison of the computing time required for the various grids was not done because lower relaxation coefficients were necessary to obtain the solutions for the more refined grids, making them even more time demanding.

Figure 5 shows the influence of the numerical scheme on the concentration front shape for three cases: *a*) Up Wind Difference Scheme (UWS); *b*) Central Difference Scheme (CDS); and *c*) Blending Scheme (50% UWS and 50% CDS). As can be observed the UWS introduces a great amount of numerical diffusion as shown by the spreading of the concentration front. On the other hand, the CDS which produces a sharper concentration front, introduces some numerical oscillations giving nom-realistic results as observed from Figure 5. Also shown in Figure 5 is a Blending Scheme, 50% UWS and 50% CDS, which produces a sharper concentration front shape without numerical oscillations.
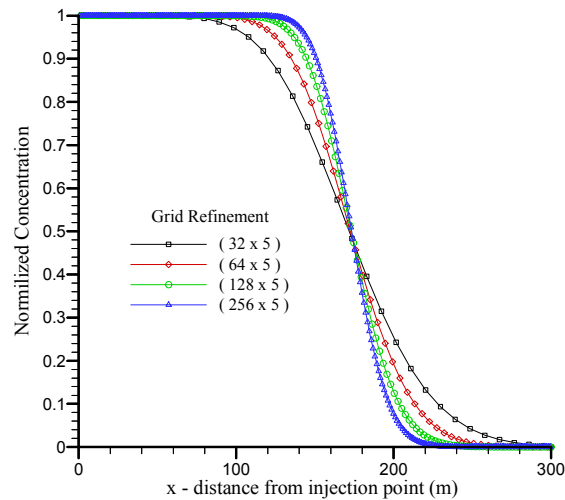
Figure 4 – Grid refinement influence on the concentration front shape (Up Wind scheme).
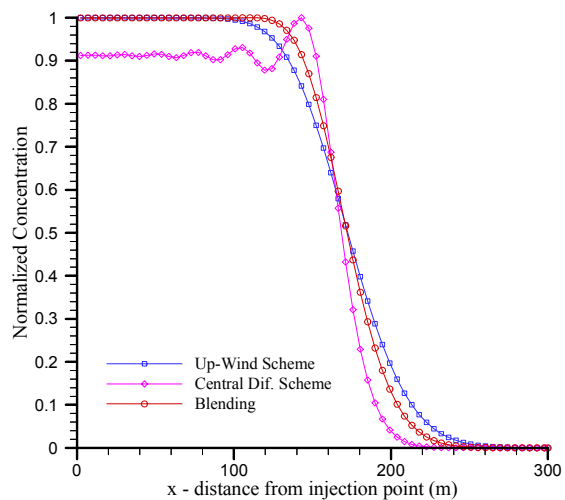
Figure 5 - Concentration Front shape for three numerical schemes (64 x 5 grid).

6. Conclusions

The problem of a tracer injection in an oil reservoir composed of two different porous regions was solved using the Finite Volume method and a single computational domain. An assessment of the numerical diffusion introduced by the grid coarseness as well as by the numerical scheme employed (UDS, CDS or Blending), was made based on the solution for a simple geometry. It was verified that, for obtaining the tracer breakthrough time, both grid refinement and numerical scheme are very important. For the grid refinement the compromise is the computing time required for very fine grids. A combination of grid refinement and numerical scheme should always be considered in such kind of problems.

7. Acknowledgments

8. References

Almeida, A. R. and Cotta, R. M., 1995, Integral Transform Methodology for Convection-Diffusion Problems in Petroleum Reservoir Engineering, *Int. J. Heat Mass Transfer*, vol. 38, n. 18, pp. 3359-3367.

Amaral Souto, H. P., Moyne, C., Murad, M. A. and Karan Filho, J., 2001, A Multiscale Approach for Heat Transfer in Solid Tumors, *Proceedings of the 2nd International Conference on Computational Heat and Mass Transfer*, Rio de Janeiro-RJ, Brasil

Amaral Souto, H. P., da Silveira, O. T., Moyne, C. and Didierjean, S., 2002, Thermal dispersion in porous media: computations by the random walk method.

de Lemos, M.J.S., Mesquita, M.S., 2003, Turtulent Mass Transport in Saturated Rigid Porous Media, *Int. Comm. Heat Mass Transfer*, vol. 30, n. 1, pp. 105-113.

de Lemos, M.J.S. and Pedras, M.H.J., 2001, Recent Mathematical Models for Turbulent Flow in Saturated Rigid Porous Media, *J. Fluids Engineering*, vol. 123. pp. 935-940.

Didierjean, S., Amaral Souto, H. P., Delannay, R. and Moyne, C., 1997, Dispersion in periodic porous media. Experience versus theory for two-dimensional systems, *Chemical Engineering Science*, vol. 52, n. 12, pp. 1861-1874.

Ochoa-Tapia, J.A. and Whitaker, S., 1997, Heat Transfer at the Boundary Between a porous Medium and a Homogeneous Fluid, *Int. J. Heat Transfer*, vol. 40, n. 11, pp. 2691-2707.

Oldenburg, C. M. and Pruess, K., 2000, Simulation of Propagating Fronts in Geothermal Reservoirs with the Implicit Leonard Total Variation Diminishing Scheme, *Geothermics*, vol. 29, pp. 1-25.

Patankar, S. V., 1980, *Numerical Heat Transfer and Fluid Flow*, Hemisphere, New York.

Pedras, M.H.J. and de-Lemos, M.J.S., 2002, Macroscopic Turbulence Modeling for Incompressible Flow Through Undeformable Porous Media, *Int. J. Heat Mass Transfer*, vol. 44, n. 6, pp. 1081-1093.

Pedras, M.H.J. and de-Lemos, M.J.S., 2000, On the Definition of Turbulent Kinetic Energy for Flow in Porous Media, *Int. Comm. Heat Mass Transfer*, vol. 27, n. 2, pp. 211-220.

Pedras, M.H.J. and de-Lemos, M.J.S., 2001a, Simulation of Turbulent Flow in Porous Media Using a Spatially Periodic Array and a Low Re Two-Equation Closure, *Numer. Heat Transfer - Part A Applications*, vol. 39, n. 1, pp. 35-59.

Pedras, M.H.J. and de-Lemos, M.J.S., 2001b, On the Mathematical Descriptions and Simulation of Turbulent Flow in a Porous Medium Formed by Array of Elliptic Rods, *J. Fluids Engineering*, vol. 123. pp. 941-947.

Quintard, M., Kaviany, M. and Whitaker, S., 1997, Two-Medium Treatment of Heat Transfer in Porous Media: Numerical Results for Effective Properties, *Adv. Water Resources*, vol. 20, pp. 77-94.

Rocamora, F.D. and de-Lemos, M.J.S., 2000, Analysis of Convective Heat Transfer for Turbulent Flow in Saturated Porous Media, *Int. Comm. Heat Mass Transfer*, vol. 27, n. 6, pp. 825-834.

Wendland, E., Risso, V. F. and Schiozer, D. J., 2001, Simulation of Two-Phase Flow in Heterogeneous Porous Media, *Proceedings of the 16th Brazilian Congress of Mechanical Engineering*, Uberlandia-MG, Brazil.